Materials Science & Engineering A 669 (2016) 75–86

Contents lists available at ScienceDirect

Materials Science & Engineering A

journal homepage: www.elsevier.com/locate/msea

Creep rupture behavior of welded Grade 91 steel

Triratna Shrestha [a], Mehdi Basirat [b], Sultan Alsagabi [a], Anumat Sittiho [a], Indrajit Charit [a,*], Gabriel P. Potirniche [b]

[a] Department of Chemical and Materials Engineering, University of Idaho, Moscow, ID 83844, USA
[b] Department of Mechanical Engineering, University of Idaho, Moscow, ID 83844, USA

ARTICLE INFO

Article history:
Received 18 August 2015
Received in revised form
16 May 2016
Accepted 17 May 2016
Available online 18 May 2016

Keywords:
Grade 91 steel
Ferritic-martensitic steel
Welding
Creep rupture
Fractography

ABSTRACT

Creep rupture behavior of fusion welded Grade 91 steel was studied in the temperature range of 600 – 700 °C and at stresses of 50–200 MPa. The creep data were analyzed in terms of the Monkman-Grant relation and Larson-Miller parameter. The creep damage tolerance factor was used to identify the origin of creep damage. The creep damage was identified as the void growth in combination with microstructural degradation. The fracture surface morphology of the ruptured specimens was studied by scanning electron microscopy and deformed microstructure examined by transmission electron microscopy, to further elucidate the rupture mechanisms.

1. Introduction

The Next Generation Nuclear Plant (NGNP) are being developed and adopted to address ever-growing energy demand and reduce CO_2 emissions. Various reactor types, such as Gas-Cooled Fast Reactor (GFR), Lead-Cooled Fast Reactor (LFR), Molten Salt Reactor (MSR), Sodium-Cooled Fast Reactor (SFR), Supercritical Water-Cooled Reactor (SCWR), and Very High Temperature Reactor (VHTR) are being considered. The VHTR is a Gen-IV reactor system at the heart of the so-called Next Generation Nuclear Plant (NGNP). The VHTRs are expected to have a 60 plus years of service life and operate at higher temperature and pressure [1]. Depending on the VHTR design, Prismatic Modular Reactor (PMR) or Pebble Bed Modular Reactor (PBMR), the operating temperature of the reactor pressure vessel (RPV) can vary between 300 °C and 650 °C. Furthermore, the RPV in the VHTR will be more than twice the size of a typical RPV in a Light Water Reactor (LWR) [2]. The RPV is considered an irreplaceable component of a nuclear power plant, which dictates its useful service life. The modified 9Cr-1Mo (Grade 91) steel is being considered for the VHTR pressure vessel material. On the other hand, the Grade 91 steel has been a material of choice in fossil-fired power plants with increased efficiency and service life, and reduction in the greenhouse gas emissions of CO_2, NO_x, SO_2, etc. The efficiency of a fossil-fired power plant depends on the temperature and pressure of the steam. The steam in these advanced coal-fired power plants is expected to have temperatures in the range of 550–720 °C and pressures above 24 MPa [3–5]. The Grade 91 steel has better erosion/corrosion resistance than traditional steels in fluidized bed combustion (FBC) boiler waterwalls and superheater tubes.

Understanding creep rupture properties of the Grade 91 steel is important for predicting the long term mechanical integrity of a power plant. Furthermore, welding is an essential manufacturing step for large power plant components. Although there are some studies on the creep-rupture properties of monolithic Grade 91 steel [6,7], there is only a limited number of studies on the creep rupture properties of the welded Grade 91 steel. Monolithic Grade 91 steel exhibited two different rate-controlling creep deformation mechanisms in the lower stress region and in the higher stress region [8]. The creep deformation mechanism in the low stress region was identified as the Nabarro-Herring creep with stress exponent of ~1, while that in high stress region was identified as high temperature dislocation climb with stress exponent of ~5 [8]. A diagnostic diagram for creep failure of monolithic Grade 91 steel showed that microstructural degradation phenomena such as particle coarsening, subgrain growth and cavity nucleation/growth played a major role in creep-rupture [6,8–12]. The fracture mechanism map of Grade 91 steel developed by Shrestha et al. [6] indicated that the monolithic samples ruptured via transgranular mode.

Welding of Grade 91 steel creates microstructural gradient across the weldment. This inhomogeneity in microstructure, mainly in the heat affected zone (HAZ), leads to type-IV cracking [13,14] and low creep strength in the fine grain HAZ (FGHAZ) [15–

* Corresponding author.
E-mail address: icharit@uidaho.edu (I. Charit).

http://dx.doi.org/10.1016/j.msea.2016.05.065
0921-5093/

Table 1.
Chemical composition (in wt%) of Grade 91 steel.

Element	Nominal	Measured
Cr	8.00–9.50	8.55
Mo	0.85–1.05	0.88
V	0.18–0.25	0.21
Nb	0.06–0.10	0.08
C	0.08–0.12	0.10
Mn	0.30–0.60	0.51
Cu	0.4 (max.)	0.18
Si	0.20–0.50	0.32
N	0.03–0.07	0.035
Ni	0.40 (max.)	0.15
P	0.02 (max.)	0.012
S	0.01 (max.)	0.005
Ti	0.01 (max.)	0.002
Al	0.02 (max.)	0.007
Zr	0.01 (max.)	0.001
Fe	Balance	Balance

19]. The exact location of type-IV cracking, whether in over-tempered martensite, FGHAZ, or inter-critical HAZ (ICHAZ), is still not settled. Partial transformation of austenite to martensite, resulting in presence of retained austenite [20], formation of delta-ferrite [21–25], and differential migration of interstitial and precipitate forming elements [26,27] across the weldment creates a complex microstructure prone to failure.

The focus of this work was to analyze the creep rupture data obtained from a fusion welded Grade 91 steel and compare them with the data obtained by authors' previous work on monolithic Grade 91 steel and with data available in literature on welded Grade 91. The previous studies by some of the current authors were focused on tensile creep properties of monolithic Grade 91 steel. Creep rupture behavior of the steel was studied and a fracture mechanism map was developed [6]. In a separate study [8] creep deformation of the steel was studied in high stress and low stress regime, whereas creep deformation of the steel was modeled using continuum-damage technique [28]. Conversely, the present study examines the creep rupture data in the light of both phenomenological and physical understanding. Specifically, an attempt has been made to analyze the data in terms of creep fracture diagnostic approach that has not been done by any contemporary work on this important steel under welded condition.

2. Experimental details

2.1. Material and welding procedure

The chemical composition of ASTM A387 Grade 91 CL2 steel (Grade 91) used in this study is given in Table 1. The hot rolled Grade 91 plates were obtained from ArcelorMittal Plate LLC, in a normalized and tempered condition (i.e., austenitized at 1038 °C for 240 min followed by air cooling and tempered at 788 °C for 43 min). The as-received plates had dimensions of 104 mm × 104 mm × 12.7 mm. The plates of aforementioned dimensions were cut into two halves and tapered on one side at 30° to make a V-butt end. Using tungsten gas arc welding (GTAW), double V-butt weld specimens were made by welding these two V-butt end halves together, as shown in Fig. 1, where Long represents the longitudinal direction, Trans represents the transverse direction, and TT the through-thickness direction. A Metrode 2.4 mm diameter 9CrMoV-N TIG filler wire having low residual elements was used for welding. The plates were pre-heated to 260 °C before welding. The steel plates were placed on an aluminum plate to prevent overheating during welding. Three successive passes were used to create the complete weld using a current of 130 A and a voltage of 15 V. Post-weld heat treatment (PWHT) of the welded plates were carried out at 750 °C for 2 h. The creep rupture tests were performed on PWHTed samples.

2.2. Microstructural characterization

Optical microscopy was performed on the as-received, welded, and creep tested specimens for characterization of the grain structure. Conventional metallographic procedures of cold mounting, grinding, and polishing were followed to prepare the specimen surface to 0.5 μm finish before etching was carried out using Marble's reagent, a solution made of 50 ml distilled water, 50 ml hydrochloric acid, and 10 g of copper sulfate. Subsequently, an Olympus light microscope was used to examine the metallographic specimens and an attached CCD camera was used to record the micrographs.

For detailed microstructural characterization, some metallographic samples were examined using a Zeiss Supra 35VP field emission gun scanning electron microscope (FEG-SEM) operated at an accelerating voltage of 10–20 kV in secondary electron imaging mode. Relevant chemical compositional analyses were performed by energy dispersive spectroscopy (EDS) technique available in the FEG-SEM. Further, transmission electron microscopy (TEM) was performed on some specific creep-tested specimens. In this regard, a JEOL 2010 J STEM was utilized at an accelerating voltage of 200 kV. The TEM sample preparation was carried out with a Fischione twin-jet electropolisher using an electrolytic solution of methanol and nitric acid (nominal volume ratio of 85:15) in a dry ice bath (about −35 °C).

Microhardness testing was carried out using a Vickers microhardness tester (LECO LM-100) where the applied load was 500 g_f (4.9 N) and the hold time 15 s.

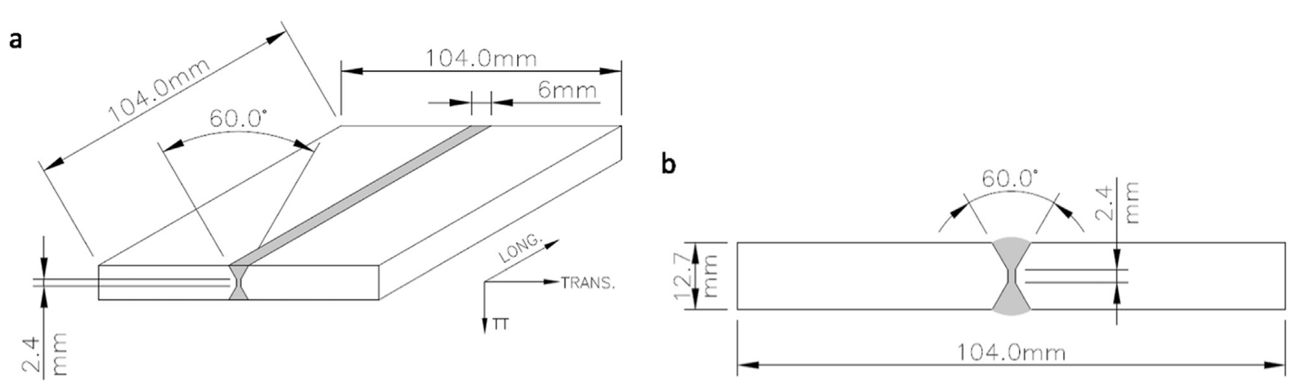

Fig. 1. Schematic representation of the double V-butt welded plate.